Mass, power and static stability optimization of a 4-wheeled planetary exploration rover

Alexandre Carvalho Leite, Bernd Schäfer

Deutsches Zentrum für Luft- und Raumfahrt, 82234 Weßling, Germany
(e-mail: alexandre.carvalholeite@dlr.de)
(e-mail: bernd.schaefer@dlr.de)

Abstract

This work focuses on a four-wheeled rover, having the NLL Rover as the main example. The chassis of the vehicle is modeled as a multi-body system (MBS), the wheel-terrain interaction permits to switch between rigid and soft soil based on the Coulombs friction model and terramechanics approach. An advantage of the MBS simulations is to evaluate the performance of the rover when the various geometric characteristics of the mechanical structure (e.g. bogie length, wheel radius) are used as design parameters. By optimizing these design parameters it is possible to achieve a lightweight structure with improved efficiency. As the main performance measures to be optimized we have identified three different ones: average consumed power, overall mass of the vehicle and static stability margin. A compromise between the design parameters could be found in order to achieve satisfying performance measure values. Animations, histograms and time-domain plots are used to evaluate the obtained results. They include the dynamic behavior of the optimized rover and the related performance measures. Two different software packages were used in our modeling/optimization procedure: Dymola (modeling environment) and Matlab/MOPS (optimization environment). The results gave us an insight about the optimization trends according with the terrain characteristics and are prone to point out the outlook of this design improvement effort, like addition of motion controllers parameters and new objective functions.

Keywords: Multiobjective optimization, multibody simulation, planetary rover, design support, contact modeling.

1. Introduction

In 2001 the European Space Agency (ESA) had initiated the Aurora Programme with its primary objective to be robotic and human exploration of the solar system. The most likely targets are Mars, the Moon and asteroids; but a manned mission is only possible after successive robotic precursor missions to test technology in-situ and gather sufficient environmental information. In this context there are two near future missions which will provide surface mobility with wheeled rovers: ExoMars and Next Lunar Lander NLL. The ExoMars Rover and the NLL Rover are powerful rovers with different capabilities under development, respectively with six and four wheels. Such vehicles that drive up rocks, loose soil and general slippery and uneven terrain often need high mobility capabilities. Modeling and design of a high-performance autonomous vehicle is generally a difficult task. Engineering requirements are even more stringent since some characteristics are highly desired but also conflicting, as light weight and high traction for example.

We understand this problem as an optimization problem with multiple criteria. The structure of the vehicle must be optimized for all-terrain navigation and several phases of its life-cycle. Some approaches in the literature provided means to evaluate vehicles with distinct configurations. In [1] a terramechanics approach was taken into account together with a set of static models relating soil and mechanical configuration of a vehicle. Kinematic models and metrics were proposed by [2] aiming at mobility evaluation of distinct mechanical configuration of vehicles. These works are based on static or kinematic models and are restricted to evaluation. We present an approach based on dynamic models capable of considering a broad range of performance criteria (static, kinematic and dynamic). This approach is not restrained to evaluation, but also employs parameter synthesis aiming at multi-objective optimization of some stated criteria. The next sections will give an overview of the multibody simulation model employed, some simulation examples, definition of objective functions and optimization results.

In section 2 the modeling of the mechanical structure as a MBS and the interaction between wheel and terrain is described through four main topics: relief pattern and coordinate system, rigid soil contact, soft soil contact and multibody simulation model. All the environmental information is contained in the wheel-terrain contact model and it is of major importance to evaluate the performance of the mechanical structure (i.e. the MBS). Section 3 focuses on simulation examples of the previously developed models. The aim of this section is to perform verification of the wheel-terrain interaction model into the MBS model of a four-wheeled rover, two examples were chosen for that purpose. Section 4 provides a description of the following optimization issues: objective functions, design parameters and multi-case optimization. The results obtained through the optimization procedure are discussed in section 5. Finally, section 6 points to the future directions of improvement of the current work.

2. Wheel-terrain contact and multibody modeling

From prior experience reported by NASAs Apollo Missions [3] and specifically by using the Lunar Roving Vehicle (LRV) on Apollos 15, 16 and 17, there is knowledge about the properties of the lunar surface [4]. Moreover, the twin vehicles of NASA's Mars Exploration Rover project drove some kilometers on the martian surface [5]; they faced a rugged land with volcanic rocks, pocked with impact craters and containing layered bedrocks distributed throughout a sandy terrain. As an abstraction of extraterrestrial terrains, our simulation model uses a contact model between wheels and an ideal rugged terrain with Coulomb friction, slippery behavior and sinkage in soft soil, impact between rigid wheels and complexly shaped stones is a feature currently under development. Either layered bedrocks or sandy terrain with regard to its relief pattern are described with variable elevation as a continuous function of the spatial location of each wheel. We compute the tangential forces at the contact as: 1) limited by the friction cone in the case of rigid soil; 2) sinkage/wheel-design dependent in the case of soft soil. Since the terrain elevations are described as a continuous function, discontinuities could only be induced by the placement of rocks with arbitrary shapes distributed according with previous knowledge as in [6]. Nevertheless, the vehicle's suspension must comply with the stringent all-terrain locomotion requirements. Note that the wheels are allowed to assume distinct elevations, for example during a traverse across steep rocky slopes in the presence of sinkage. From the designer's point of view, the simulation model of a suspension system should also be able to change its geometric parameters aiming to achieve a better performance under a given landing site.

The contact model is explained in subsections 2.1-2.3, the shape of the terrain and the forces developed at the contact patch of rigid wheel in contact with rigid and soft soil are itemized. Subsection 2.4 gives a short description about the MBS modeling tools and methods employed.

2.1 Relief pattern and coordinate system

Regarding the relief pattern, it is valid either for rigid or soft soils and defined at the contact patch of each wheel of a multi-wheeled planetary exploration rover. A three-dimensional surface in the form $z = f(x, y)$ is a scalar field used to compute the orientation of the contact's normal vector e_n, where (x, y) are points of the plane and z the respective terrain elevation, see figure 1a.

The rotation axis of the wheel e_{axis} follows the attitude of the wheel, this is used to determine the longitudinal direction ($e_{long} = e_n \times e_{axis}$) of the contact point's coordinate system. The right-handed coordinate system is completed with the lateral direction as $e_{lat} = e_{long} \times e_n$. In this way the coordinate system of the contact point of the wheel is locally defined as a function of the terrain and orientation of the wheel. The normal vector is the direction where the normal force is computed; longitudinal and lateral vectors are in the tangent plane, where the traction force and motion resistance forces occur. Figure 1b is an example of a four-wheeled vehicle on a Gaussian-shaped terrain.

2.2. Rigid soil contact

To compute the normal force the penalty method is used. It consists of a compliant system giving forces that are proportional to violation of constraints to solve the constraints, the forces are computed in the normal and tangent direction by spring-damper model [8], which can be linear or non-linear. Equations (1) is the general form of the normal force computation and equation (2) is the general form of the tangential force vector computation.
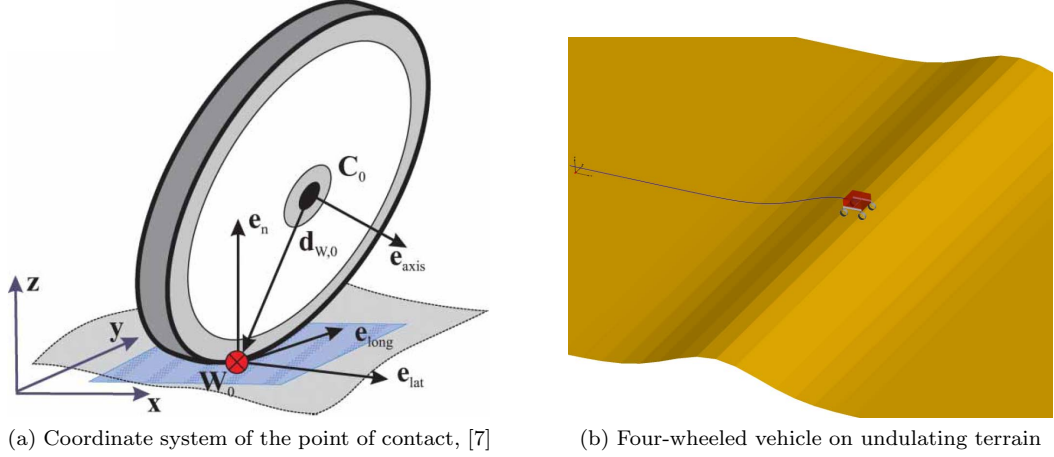
(a) Coordinate system of the point of contact, [7]

(b) Four-wheeled vehicle on undulating terrain

Figure 1: Coordinate system's definition and example

$$F_N = f_{N,i}(\delta_{N,i}) + g_{N,i}(\delta_{N,i}, \dot{\delta}_{N,i}) \tag{1}$$

$$\mathbf{F_T} = f_{T,i}(\delta_{\mathbf{T,i}}) + g_{T,i}(\delta_{\mathbf{T,i}}, \dot{\delta}_{\mathbf{T,i}}) \tag{2}$$

Where the terms $f_{N,i}(.)$ and $f_{T,i}(.)$ are representing the springs, the terms $g_{N,i}(.)$ and $g_{T,i}(.)$ are representing the dampers, $\delta_{N,i}$ and $\delta_{\mathbf{T,i}}$ are the corresponding displacements of the spring-damper system with its respective time derivatives $\dot{\delta}_{N,i}$ and $, \dot{\delta}_{\mathbf{T,i}}$. At this stage we have a kinematical problem with additional states, this is justified by the avoidance of the static indeterminacy of the normal forces on a multi-wheeled vehicle. This is a reasonably quick and accurate solution, but a problem resides in the fact that only the most penetrating point is taken into account. This point can change very quickly, appear and disappear causing discontinuities not easily treated by the simulation tool. Its apparent simplicity becomes a problem when contact areas instead of contact points are present. A quick and accurate contact model is being prepared to solve this problem and get smoother behavior of the normal forces in face-face contacts. The forces developed on the tangent plane are based on Coulomb's model including pure rolling and slippery behavior. The implementation of the Coulomb's friction model is not a simple task in our simulation/modeling tool (Dymola), since the order of the system of DAEs (Differential Algebraic Equations) changes during the simulation. In other words, it becomes a variable-structure system and can be approached in different ways. In [9] a solution with an approximation of the friction cone by a friction pyramid is proposed by means of a Linear Complementarity Problem (LCP) formulation, with that assumption the solution is always possible. A regularized Coulomb friction is extensively used [7] to get a continuous and easily tractable version of the Coulomb model, the weakness of this approach is in the zero-crossing in the region of zero-slip (this is reasonable if one assumes that there is no zero-slip situation). Another solution proposed in [8], applied previously in [10] and also adopted here, uses a compliant system to compute the tangential forces inside the friction cone with a little amount of slip allowed between rolling-slipping transitions and vice versa. In this approach, the 2-dimensional spring-damper is required to maintain the nonholonomic rolling constraint until the maximum force μF_N is reached. In this moment the 2D spring-damper can change its direction but its displacement is limited by a circle with the radius proportional to μF_N, see figure 2.

Despite the advantages of the compliant model for the tangential forces, the success of this scheme is sensitive to the parameters of the spring, damper and also sensitive to the equation used to model the spring-damper system. It would not be a problem for a fixed configuration of a planetary rover, i.e. fixed dimensions of the mechanical structure. But since the mechanical structure is changed for each simulation run during the optimization procedure, these parameters must be suitably changed or even fixed in order to accurately comply with each new scenario (rover parametric configuration plus terrain characteristics). Nevertheless there are means to work round unwanted results, the simulation conditions can be fixed and greatly contribute to accommodate simulation stability during the overall optimization process. Another solution would be synthesize those parameters by means of optimization algorithms for extreme rover geometric configurations of a given kinematic in given terrains. It would be a multi-model multi-case approach applied to the tuning of simulation-related parameters. The criteria for this tuning
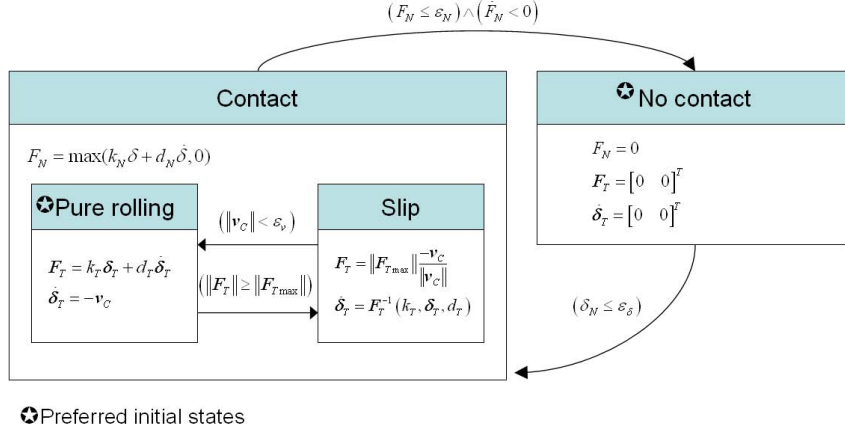
$$\left(F_N \leq \varepsilon_N\right) \wedge \left(\dot{F}_N < 0\right)$$

Contact

$$F_N = \max(k_N \delta + d_N \dot{\delta}, 0)$$

✿Pure rolling

$$F_T = k_T \delta_T + d_T \dot{\delta}_T$$
$$\delta_T = -v_C$$

$$\left(\|v_C\| < \varepsilon_v\right)$$

$$\left(\|F_T\| \geq \|F_{T\max}\|\right)$$

Slip

$$F_T = \|F_{T\max}\| \frac{-v_C}{\|v_C\|}$$
$$\dot{\delta}_T = F_T^{-1}(k_T, \delta_T, d_T)$$

✿No contact

$$F_N = 0$$
$$F_T = \begin{bmatrix} 0 & 0 \end{bmatrix}^T$$
$$\delta_T = \begin{bmatrix} 0 & 0 \end{bmatrix}^T$$

$$\left(\delta_N \leq \varepsilon_\delta\right)$$

✿Preferred initial states

Figure 2: State transitions of the frictional contact model

process would be "simulation robustness" metrics (e.g. "chattering", simulation time and numerical instability). This last solution will be implemented in a future version of our rover optimization framework.

2.3 Soft soil contact

The soft soil contact is simulated according with the well known Bekker's equations [11]. The equations used here were obtained from the simplified version of [12], they permit a faster calculation of the sinkage and entry angle. The propeling force (also known as tractive thrust) is subtracted by the motion resistance forces: compaction, bulldozing and gravity's influence on inclined slopes. The force diagram acting on a wheel is in figure 3a, where σ is the normal pressure acting radially on the wheel rim, θ_0 is the entry angle, θ is the angular position coordinate of the wheel-soil contact as counted forward from the wheel bottom dead-center, z_0 is the maximum sinkage at the bottom-dead-center, W is the vertical load acting on the wheel and D is the diameter of the wheel. Figure 3b shows the constant of approach α which is constant and used to calculate the bulldozing resistance according with [11].

(a) Geometry and forces for a single rigid wheel on soil

(b) Definition of angle α for determination of bulldozing resistance
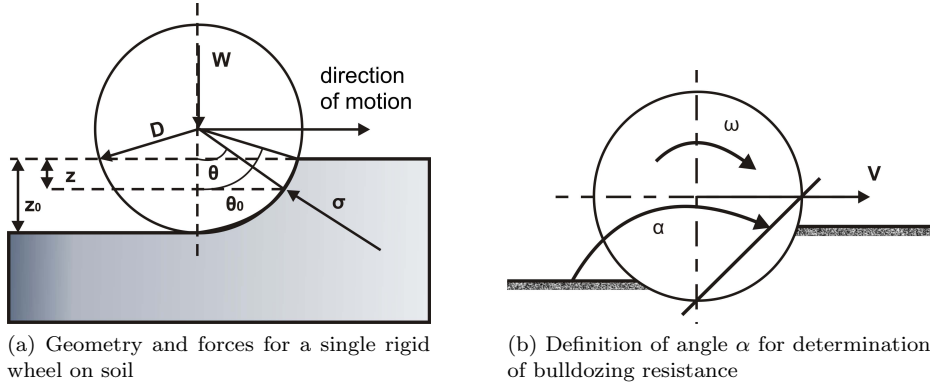
Figure 3: Diagrams of terramechanics

In figure 4a, the drawbar pull of the vehicle simulated in Dymola at the same conditions as the corresponding experiment with the ExoMars breadboard chassis (see figure 4b) tests are presented as a function of slippage for the same soil characteristics (Bekker parameters) as in [13]. Note that the force measurements were horizontally strongly compressed and placed close to the corresponding slippage value in the diagram, [14].

Other soft soil contact models are currently in development to achieve more precise experimental results, they are also based on Bekker's equations but not simplified. Furthermore, advanced methods as in [16] and [17] based on tetrahedral meshes and particle-based simulation of granular materials are also encouraged as future attempts in describing precisely soil-wheel interactions.

2.4 Multibody simulation model
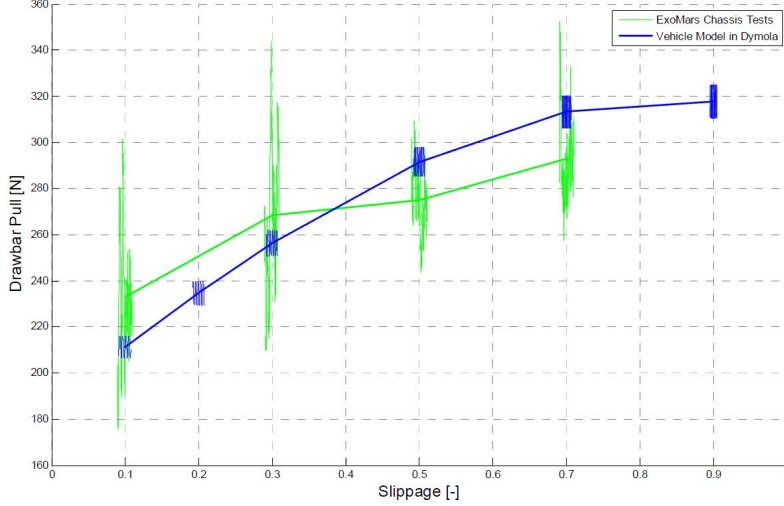
(a) Drawbar pull versus slip comparing simulation and experiment with the ExoMars rover breadboard model

(b) Illustration of a drawbar pull experiment from [15]

Figure 4: Model validation

We used Dymola as modeling and simulation tool. The kinematic of the vehicle was modeled by multibody components available on a standard package of Dymola, they are basically revolute joints, fixed connections and rigid bodies, see figure 5.
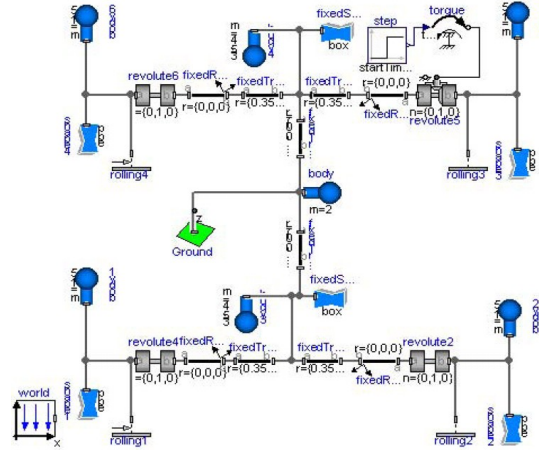

Figure 5: Multibody model of the four-wheeled rover

Once defined, the geometry of the mechanical structure is fully parameterizable. The MBS is scalable, environmental aspects and contact models can be freely included to define the desired physical constraints. Additions can be inserted by means of Modelica language directly interpreted by Dymola, or through external functions from libraries specifically coded for that purpose. In the current version it was completely implemented in Modelica language, but a new version under development calls external functions to speed-up some computations and detect contact between wheels and rocks.
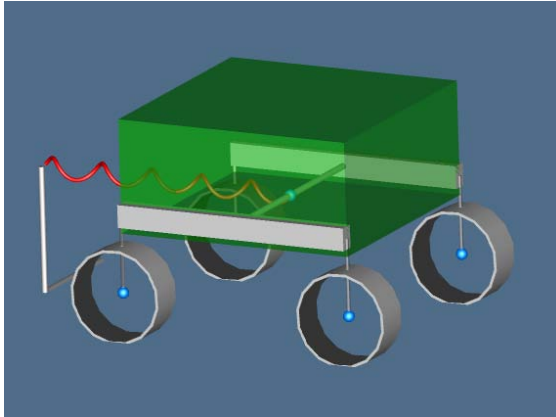
3. Simulation

Our contact models are verified by means of simulation. The MBS model is coupled with the rigid/soft contact models for each wheel in order to: 1) evaluate if the model is behaving as expected; 2) gather knowledge about the robustness and stability of the numerical results as it influences the optimization process. The first objective can be simply considered as a basic stage of checking for implementation errors and seek more efficient implementation schemes to speed up the duration of the simulation. The

second objective is strictly related with our optimization procedure, because each optimization iteration require one simulation run. It means that the simulation model must be capable of providing reliable results not only for one scenario (rover parametric configuration plus terrain characteristics), but as many as the optimizer arbitrates.

The contact model is inserted as an interface for each wheel of the planetary rover with the terrain. We also defined two simulation examples to underline some observations about the objectives stated at the beginning of this section. The error checking and robustness/stability analysis of the rigid soil contact model is entrusted to the first example, which must explore the switching between the states and meta-states as shown in figure 2. A hybrid system can be burdensome for our simulation environment because it generate state events and they are potential sources of discontinuities and chattering. Both effects are undesirable since they can stop the simulation or make it extremely slow. In the case of the soft soil contact model, sinkage is very important in the computation of the resistance forces and depends on slippage, load on a wheel and multipass effects. Its computation is evaluated on an uneven terrain, where the load on the wheels are constantly changed. In this way plausibility can be checked and the response to the initial conditions analyzed to point a suitable initialization algorithm.

The first example is defined as follows: a spring is attached to the rover as in figure 6a, and the rover starts to pull the spring at $10s$ following a ramp-like profile until $20s$. Figure 6b shows the force delivered by the spring when it is stretched, the curve is linear during almost the whole simulation. The force curve of the spring changes only in the rolling-slipping and slipping-rolling transitions. Traction force in figure 6c is limited by μF_N. There is an unrealistic slippery behavior in the first seconds of simulation (see figure 6d), this is due to the initialization of the simulation, where the thresholds are relaxed to assure initialization of the normal forces, since they cannot be statically determined. The transient slip at $10s$ in figure 6d is one characteristic of the compliant system, this can be decreased or softened by changing the spring and damper constants. When the vehicle achieves the maximal allowed traction by the soil at approximately $86s$ in figure 6c, the vehicle starts to slip until the end of the simulation as seen in figure 6d.
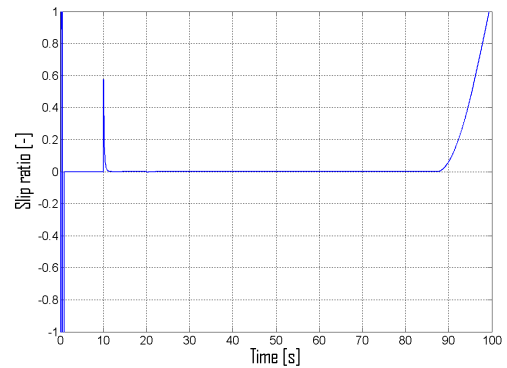

(a) Animation of the simulation
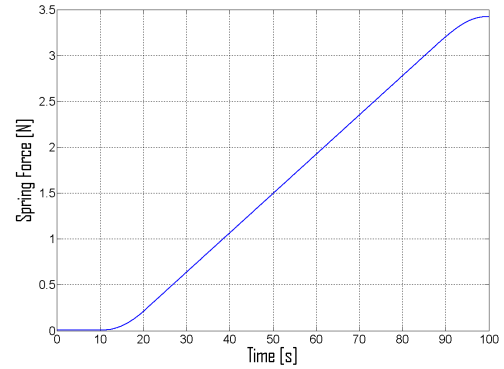
(b) Spring force
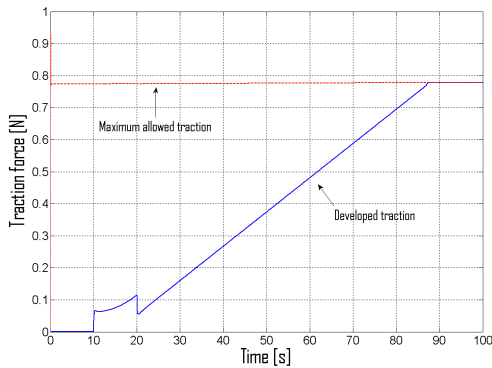
(c) Traction calculated by the Coulomb model

(d) Slippery behavior with the compliant system

Figure 6: Simulation results of the frictional contact model with the rover pulling a spring

The second example is the rover traversing a sand hill. Figure 7a shows the front and rear wheels driving up the hill slower then they drive down. When they drive up, the normal forces in figure 7b are higher in the rear wheels and the situation changes in downhill motion. Note in figure 7c that the rear wheels sinks further down because of the track left by the front wheels.

From the first example, we derived conditions to simulate a rigid terrain into an useful scope (i.e. spring-damper constants, compliant system equations and terrain unevenness) where the simulation is robust and stable for bounded values of the design parameters set by the optimizer. From the second example, we derived a time triggered initialization algorithm to properly accommodate the state vector of the system and guarantee plausible starting values on a displaced starting time. Within the stated conditions, the MBS model and its respective wheel-terrain interfaces can be employed into the optimization procedure.
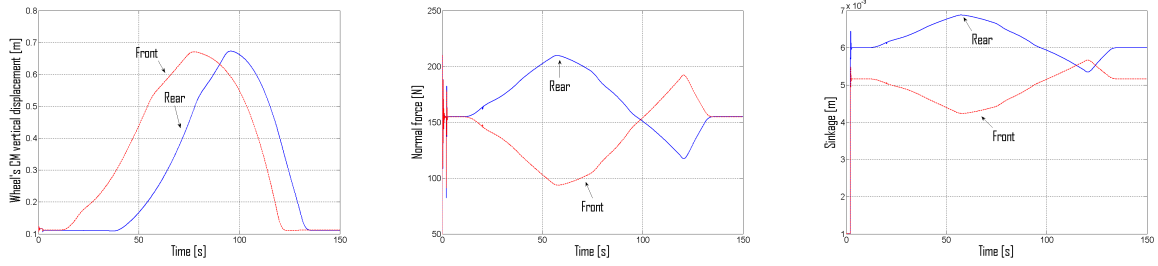
(a) Displacement of the center of mass of the front and rear wheels

(b) Normal forces in the front and rear wheels

(c) Soil sinkage in the front and rear wheels

Figure 7: Simulation results of the soft soil contact model with the rover traversing a sand hill

4. Optimization

Each simulation run can be viewed as a part of one iteration of the optimization process. After each simulation run the objective functions are computed, the parameters of the mechanical structure are tuned in order to track the desired values of the objective functions. This process must be performed to concurrently fulfill objectives in different cases. The next sections detail the optimization scheme, some results are presented and discussed in the sequence as well as suggestion and hints of improving features which are under development.

4.1 Objective functions and design parameters

MOPS allows the definition of objective functions as: equality constraints, inequality constraints or functions to be minimized. It understands fulfillment of constraints as objectives to be reached, not only minimization of a given function but also to keep constraints under a pre-specified bound. One can define either constraints or functions to be minimized with demand values or bad-good values.

$$\hat{c}_k (T) = \frac{c_k (T)}{d_k} \tag{3}$$

The k-th objective function (also called criterion) c_k scaled with a demand value d_k, as in equation (3), satisfied the specification only when its value is less than one. Thus $\hat{c}_k(T)$ is the scaled criterion depending on the vector T of parameters. An example of 'good-bad' value for the criterion of overall mass is given in figure 8. In this case, values below the 'good-high' limit (6kg) are considered good and no additional improvement is needed. Values between 6kg and 15kg are acceptable but can be improved. The values greater than 15kg must be improved to achieve the requirement (i.e. to belong to the acceptable or good region).

The design parameters are seven: track of the vehicle, wheel width, wheel diameter, wheel thickness, bogie cross-sectional area, bogie length and wheel-bogie distance, see figure 9.

The parameter vector presented in equation (3) is now expressed by $T = [d_w \ b_w \ d_v \ b_v \ d_{wb} \ t_w \ A_b]^T$ and is changed during the optimization process at the end of each simulation run. The objective functions adopted in this work are three: overall mass, average power consumption and static stability; computed respectively as in equations (4)-(6).
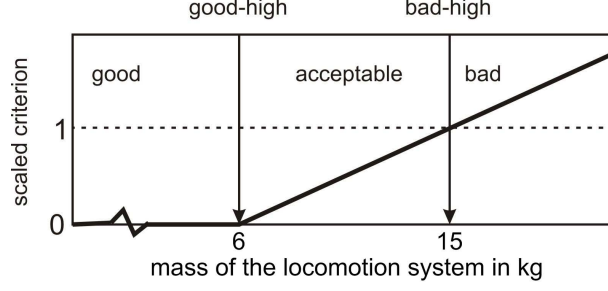
7

Figure 8: An example of 'bad-good' scaling

d_v	Track of the vehicle
b_v	Length of the vehicle
d_w	Diameter of the wheel
b_w	Width of the wheel
d_{wb}	Bogie-wheel distance
t_w	Wheel thickness
A_b	Cross-sectional area of the bogie

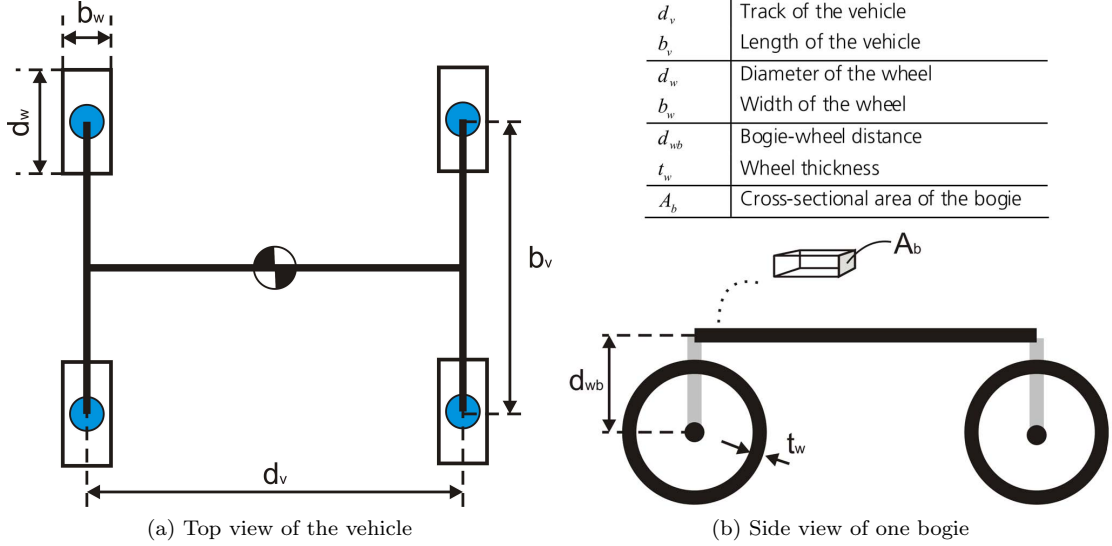(a) Top view of the vehicle (b) Side view of one bogie

Figure 9: Visual description of the tuning parameters in vector T

$$J_{mass} = \sum_{parts} m_{parts} \qquad (4)$$

$$J_{avpower} = \sum_{wheels} \frac{1}{\Delta t} \int_0^{\Delta t} |\tau \cdot \omega| \ dt \qquad (5)$$

$$J_{stability} = \min\left(lateral, longitudinal\right) \qquad (6)$$

Note that the second objective function depends on dynamic simulation, and the other two can be computed without numerical integrators. The first objective function (4) is the overall mass of the locomotion system, which excludes the payload by considering only the sum of the mass of each part of the locomotion system. In (5) the average power dispended in one specific traverse is computed, Δt is the simulation time and τ and ω are torque and angular velocity of one of the wheels. The third objective function (6) assumes that the vehicle can tipover in lateral and longitudinal directions, the lowest stability boundary is taken as a measure of the static stability of the vehicle. It means that the worst (minimum) of the longitudinal and lateral stability margins must be maximized. Overall mass and average power should be minimized and static stability margin maximized. Each metric in equations (4)-(6) has a correspondence to one of the criteria c_k. The last metric can be further improved by using the support polygon approach as in [2], this is a more realistic approach since it is able to handle any kind of vehicle footprint at any angle relative to the slope by considering the outermost wheel-terrain contact points.

4.2 Multi-case optimization

A robust set of parameters can be found by using the multi-case approach. For example, for computational models depending on other parameters which are uncertain (like terrain characteristics), the

8

robustness against terrain parameter variations can be achieved by trying to apply a unique mechanical structure to a whole set of model instantiations, corresponding to different values of physical parameters of the terrain.

A multi-objective optimization scheme can be applied in several cases (e.g. lunar soft soil, martian soft soil, rigid surface, mixed soft and rocky surface) in the same procedure. In other words, at the end of the optimization procedure one obtains a set of parameters synthesized to achieve multiple-objectives not in only one operating condition but several, which are inside the scope of the project.

This is very important for mobility of all-terrain robots, since the terrain has frictional, terramechanical and rock distribution characteristics which are uncertain and to which the objective functions are highly sensitive.

4.3 Optimization method

MOPS provides several optimization routines, see [18]. The best results in this work was achieve by the Differential Evolution method.

Differential Evolution (DE) is a method of mathematical optimization of multidimensional functions and belongs to the class of evolution strategy optimizers. DE finds the global minimum of a multidimensional, multimodal function with good probability. The crucial idea behind DE is a scheme for generating trial parameter vectors. DE adds the weighted difference between two population vectors to a third vector. For the first time Differential Evolution was described by [19].

The implementation in MOPS is based on the free distributed software by [19] and is adapted for parallel computation of the populations. Furthermore the MOPS implementation of DE is extended by a hybrid (combined global/local) optimization feature and differs in the termination policy. Linear or non-linear constraints are addressed by the exact L1-Penalty function.

5. Results

The geometrical parameters of the mechanical structure of the rover were synthesized using the optimization algorithms package implemented in MOPS. A Pareto-optimal or 'non-inferior' solution is adopted as criterion to make decisions against conflicting objective functions. Table 1 shows the parameter vector found by the differential evolution algorithm compared with the start values. The set of values complies with the three stated objective functions. *Nominal* means starting configuration, its geometric parameters were arbitrarily chosen based on previous experience with the optimization of the ExoMars rover in [14].

Table 1: Numerical results of the optimization process

Rover	d_w	b_w	d_v	b_v	d_{wb}	t_w	A_b
Nominal	0.25m	0.10m	0.64m	1.27m	0.205m	7.5×10^{-3}m	2.4×10^{-3}m^2
Optimized	0.25m	0.06m	0.80m	1.90m	0.140m	2.6×10^{-3}m	1.2×10^{-3}m^2

All the objective functions could provide satisfactory results for the simulated conditions in rigid and soft soil. Figure 10 shows the percentage improvement of mass, static stability and average power. Improvement in mass and average consumed power means reduction, in static stability it means an increase of the static stability margin. These results were evaluated for other variations of terrains and the optimized version could achieve a reduction of 45% of average consumed power driving in soft soil when compared with the nominal rover.

Figure 11 gives an overview of the optimized and nominal solutions. Note that the optimized rover has thinner wheels and this is not a good choice for soft soil navigation. Simulations in soft soil confirmed an increase in sinkage and slippage.

In this optimization procedure, stringent demand values were chosen for the objective functions. The demand values handle the compromise (Pareto-optimal) solutions based on designer priorities. If all the objective functions comply with the demand values, they must be located inside the unity cube of figure 12. One can see that different optimization algorithms were able to achieve certain locations in the objective functions space, the differential evolution algorithm could find the best compromise among the
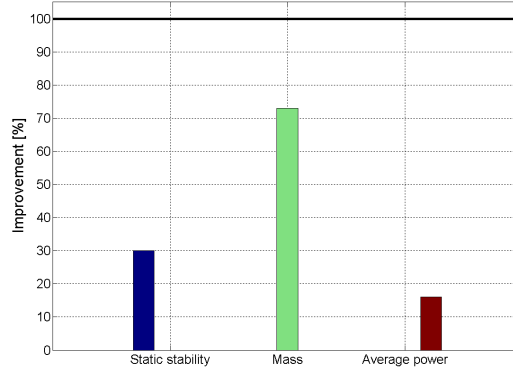
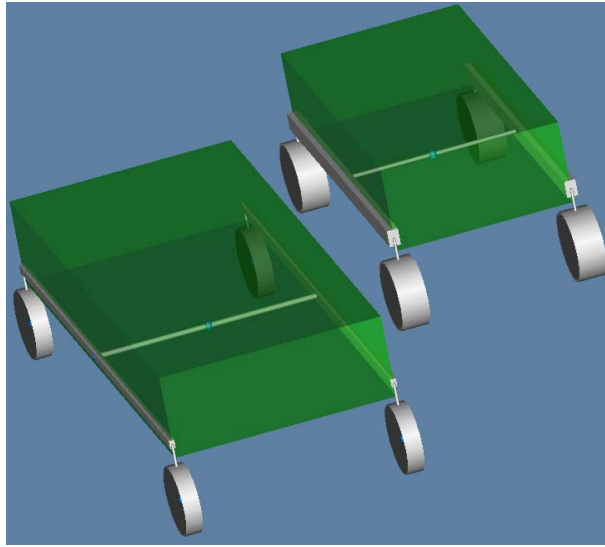Figure 10: Percentage of improvement in each objective function

Figure 11: Comparison of the optimized (left) and nominal (right) rovers

stated objective functions.

6. Conclusion and outlook

This work stated an optimization problem dealing with three objective functions. The application example was quite simple, but can become very time consuming because of the batch simulations which must be performed. Our simulation model has its complexity continuously increased with the compromise of keeping it fast. The number of objective functions may be increased, since there are other characteristics very important for a planetary exploration mission. Sinkage and slippage are two characteristics which can be included as new objective functions with its respective metrics well defined. The final solution was evaluated in several relief patterns of rigid and soft soils and gave satisfactory results of average consumed power, that is the only objective function computed by means of numerical integration.

The solution is very sensitive to the contact models. Since the kinematic configuration of the mechanical structure is immutable, the objective functions became strongly influenced by the environmental conditions. A sensitivity analysis can be performed in such a way to relate objective functions with terrain characteristics and not only with the tuners, as usual.

An important extension of this work would be the inclusion of new objective functions coping with trafficability aspects and the analysis of sensitivity. It could provide directions to recommend effective tuning parameters and admissible terrain characteristics. The time-varying quantities (i.e. slip, sinkage and power) can also be further improved by appropriate optimization of the motion controllers. As a
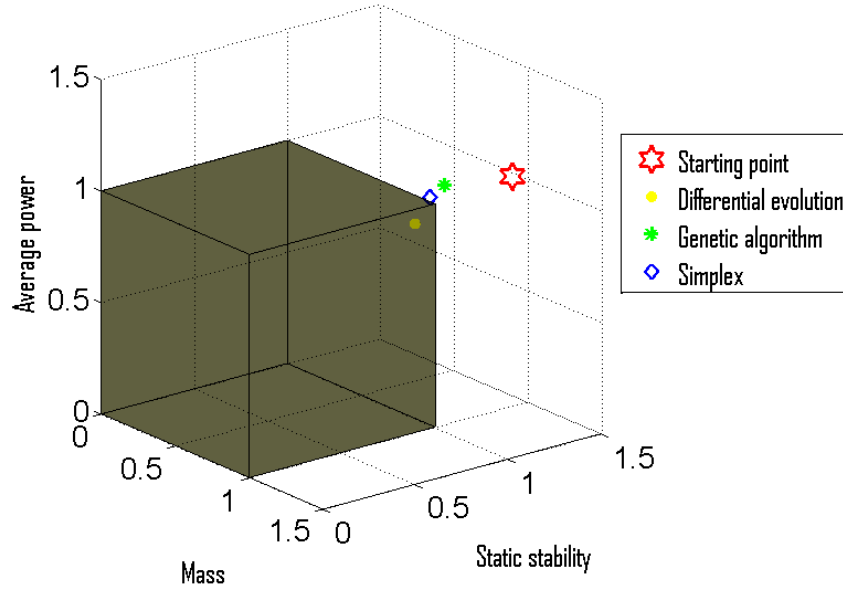
Figure 12: Unity cube in the normalized objective functions space

matter of methodology, it can be employed on a previously optimized mechanical structure.

References

[1] D. S. Apostolopoulos. *Analytical Configuration of Wheeled Robotic Locomotion*. PhD thesis, Carnegie Mellon University, Pittsburgh, Pennsylvania, 2001.

[2] T. Thüer. *Mobility evaluation of wheeled all-terrain robots*. PhD thesis, Eidgenössische Technische Hochschule Zürich, Zurich, Switzerland, 2009.

[3] Mission Evaluation Team. Apollo 14 mission report. Technical Report MSC-04112, NASA, Houston, Texas, May 1971.

[4] Grant H. Heiken, David T. Vaniman, and Bevan M. French. *Lunar sourcebook - a user's guide to the moon*, chapter 9, pages 475–567. Cambridge University Press, 1991.

[5] Jet Propulsion Laboratory. Mars exploration rover. *NASA Facts*, October 2004.

[6] M.P. Golombek. Rock statistics calculations for the mer landing sites. In *3rd MER Landing Site Workshop*, March 2002.

[7] Dirk Zimmer and Martin Otter. Real-time models for wheels and tyres in an object-oriented modelling framework. *Vehicle System Dynamics*, 48:189–216, February 2010.

[8] P. R. Kraus, A. Fredriksson, and V. Kumar. Modeling of frictional contacts for dynamic simulation. In *IROS 1997 Workshop on Dynamic Simulation: Methods and Applications*, September 1997.

[9] Jeff Trinkle, Jong shi Pang, Sandra Sudarsky, and Grace Lo. On dynamic multi-rigid-body contact problems with coulomb friction. *ZAMM - Journal of Applied Mathematics and Mechanics / Zeitschrift für Angewandte Mathematik und Mechanik*, 77:267–269, November 2006.

[10] G. Sohl and A. Jain. Wheel-terrain contact modeling in the roams planetary rover simulation. In *2005 ASME International Design Engineering Technical Conference*, Long Beach, California, September 2005.

[11] M. G. Bekker. *Theory of Land Locomotion*. The University of Michigan Press, 1956.

[12] L. Richter, A. Ellery, Y. Gao, S. Michaud, N. Schmitz, and S. Weiß. A predictive wheel-soil interaction model for planetary rovers validated in testbeds and against mer mars rover performance data. In *European Planetary Science Congress 2006*, Berlin, Germany, September 2006.

[13] B. Schäfer, A. Gibbesh, R. Krenn, and B. Rebele. Planetary rover mobility simulation on soft and uneven terrain. *Vehicle System Dynamics*, 48:149–169, January 2010.

[14] Alexandre C. Leite and Bernd Schäfer. Multibody modeling and multi-objective optimization of a six-wheeled steerable vehicle and its motion controllers. In *1st ESA Workshop on Multibody Dynamics for Space Applications*, Noordwijk, Netherland, February 2010.

[15] S. Michaud, M. Höpflinger, T. Thüer, C. Lee, A. Krebs, B. Despont, A. Gibbesh, and L. Richter. Lesson learned from exomars locomotion system test campaign. In *10th ESA Workshop on Advanced Space Technologies for Robotics and Automation - Astra*, Noordwijk, Netherland, November 2008.

[16] Yongning Zhu and Robert Bridson. Animating sand as a fluid. In *SIGGRAPH '05: ACM SIGGRAPH 2005 Papers*, pages 965–972, New York, NY, USA, 2005. ACM.

[17] Nuttapong Chentanez, Bryan Feldman, Franois Labelle, James O'Brien, and Jonathan Richard Shewchuk. Liquid simulation on lattice-based tetrahedral meshes. In *Symposium on Computer Animation*, San Diego, California, 2007.

[18] H. H. Joos. Mops multi-objective parameter synthesis user's guide v 5.3. Technical Report DLR IB 515-08-37., 2008.

[19] R. Storn and K. Price. Differential evolution - a simple and efficient adaptive scheme for global optimization over continuous spaces. Technical Report TR-95-012, ICSI, March 1995.